The design of the apodizing functions for guided-wave EOTF

Jing Zhou (周 静)

Department of Physics, Beijing Normal University, Beijing 100875

Received August 5, 2002

A design method of the apodizing functions for guided-wave four-port electrooptic tunable filter (EOTF) is proposed. As an example, the specific form of Gaussian apodizing function is designed by analyzing the crosstalk performance of EOTF. Crosstalk is calculated based on the transient response of the filter to an input optical pulse. It is concluded that crosstalk level below −30 dB for 20-Gb/s data rates and 100-GHz channel spacing is achievable with presently available substrate dimensions.

OCIS code: 060.2340.

Tunable channel-dropping filter is an important component for wavelength division multiplexing (WDM). Many guided wave filter approaches are at various stages of development, including the fiber Bragg grating[1,2], fiber Fabry-Perot[3,4], asymmetrical Mach-Zehnder interferometer (MZI)[5,6], waveguide grating router(WGR)[7,8], acoustooptic tunable filter (AOTF)[9,10], and electrooptic tunable filter (EOTF)[11,12]. Among these technologies, only the EOTF can be tuned from one channel to another at the sub-microsecond speeds needed for fast packet-switched network. Other favorable attributes of the EOTF include polarization independence and low electrical power dissipation. However, crosstalk remains a critical issue. For the EOTF to be widely used, it must at least provide acceptable interchannel crosstalk values with a channel spacing equal to the international standard of 100 GHz (0.78 nm at 1.53-μm wavelength) at 1-Gb/s data rates (OC-192, STM-64).

In this paper, the apodized EOTF design is treated theoretically to improve the crosstalk performance. Dependence of crosstalk on input pulse width is calculated for Gaussian apodizing function.

The EOTF structure considered is a four-port device that performs the add-drop function for multiple wavelength channels. It consists of two polarizing beam splitters (PBSs) connected by single mode optical waveguide sections, as illustrated in Fig. 1. Each of these waveguide sections is integrated with a spatiallyperiodic strain-inducing film[12] for inducing TE-TM polarization conversion that, by design, is efficient only for a narrow band of frequencies near the selected frequency ν_s. This allows for somewhat better crosstalk performance than in the "dual-electrode" version[11] for a given device length. The input PBS separates the TE and TM polarized components of input light and routes them through the different polarization conversion waveguide sections. The output PBS recombines light from the two waveguides so that polarization-converted light emerges from one output port (drop port), while unconverted light emerges from the other output port. The analysis here focuses on the limitations of the crosstalk related to polarization conversion in the waveguides, and assumes with ideal PBS performance.

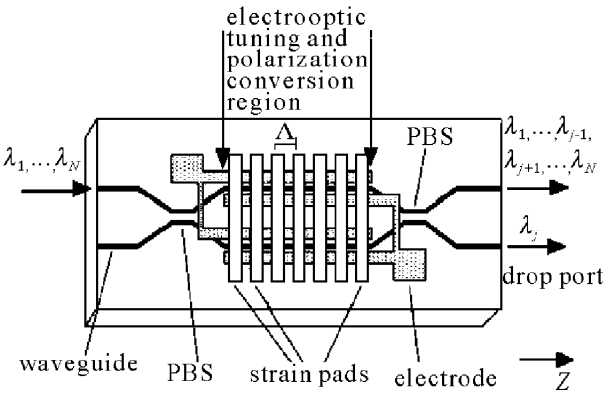

Fig. 1. Model design for EOTF.

Tuning of the filter is accomplished by applying a voltage to electrodes positioned on either side of the waveguides in the polarization conversion regions. Via the linear electrooptic effect, the voltage affects the birefringence of the waveguides, which determines the filter's selected frequency.

The analysis assumes that an optical pulse is injected into an input port and computes the temporal dependence of optical power at the output port corresponding to the selected channel. The carrier frequency of the pulse ν_0 corresponds to the center of one of the frequency channels. The crosstalk X is defined as the ratio of the optical output energy $W_{\rm out}^{\rm ns}$ if the input is in a nonselected channel to the output energy $W_{\rm out}^{\rm s}$ if the input is in the selected channel. The same input pulse waveform is assumed in both cases

$$X = \frac{W_{\rm out}^{\rm ns}}{W_{\rm out}^{\rm s}}. \tag{1}$$

The insertion loss I is defined as the ratio of $W_{\rm out}^{\rm s}$ to $W_{\rm in}$, with $W_{\rm in}$ the input optical power.

The calculation makes use of the frequency-domain transfer function $T(\omega)$ of the filter. The frequency domain response $G(\omega)$ to an input pulse of amplitude $f(t)$ is given by $G(\omega) = F(\omega)T(\omega)$, with $F(\omega)$ the Fourier transform of $f(t)$. The output pulse amplitude $g(t)$ is given by the inverse Fourier transform of $G(\omega)$.

The filter transfer function $T(\omega)$ is calculated using the coupled mode equations[13]

$$\frac{{\rm d}A}{{\rm d}z} = \kappa_{ab} B {\rm e}^{-i\Delta z}, \tag{2}$$

$$\frac{\mathrm{d}B}{\mathrm{d}z} = \kappa_{ba} A \mathrm{e}^{+i\Delta z}, \tag{3}$$

where A and B are the complex amplitudes of the two orthogonally polarized waveguide modes with different propagation constants β_a and β_b, and Δ is the phase-mismatch constant for first-order coupling.

The constants κ_{ab} and κ_{ba} in Eqs. (2) and (3) are coefficients which describe the strength of coupling between polarization modes. For the co-directional coupling, as in the present case, we can write $\kappa_{ab} = -\kappa_{ba}^* = \kappa$. For an apodized filter designed to minimize sidelobes, κ is a function of z: $\kappa(z)$, which is called the apodizing function. In designing the EOTF, we solve Eqs. (2) and (3) numerically over the region $0 \le z \le L$ to get a proper form of $\kappa(z)$ at a particular optical radian frequency ν.

In the low-crosstalk filter designs, we considered Gaussian coupling strength function, given by

$$\kappa(z) = \kappa_0 \mathrm{e}^{-\alpha^2 (z - \frac{L}{2})^2}. \tag{4}$$

The constants κ_0 and α can be adjusted in an effort to achieve a desired filter response.

The input pulse amplitude, assumed to have Gaussian shape, can be expressed as

$$f(t) = N \mathrm{e}^{-\frac{t^2}{2T_0^2}} \mathrm{e}^{i\omega_0 t}, \tag{5}$$

where N is the normalization constant, T_0 is a constant that determines the pulse width, and ω_0 is the radian frequency of the optical carrier. It is assumed that ω_0 coincides with the center of one of the WDM channels.

The calculations are intended to relate to present-day WDM system application. Thus, we consider applications of the EOTF at data rates of 2.5, 10, and 20 Gb/s. The channel spacing is assumed to be 100 GHz, and the center wavelength is 1.53 μm. Length of the electrooptic/polarization coupling region in the filter is assumed to be 6 cm, which is compatible with the 10-cm diameter of the largest commercially available lithium niobate substrates.

The birefringence of lithium niobate at room temperature for the wavelength of 1.53 μm is 0.079[14]. The constants in the apodizing function $\kappa(z)$ in Eq. (4) were determined by minimizing the crosstalk subject to the constraint that the insertion loss vanishes for $\nu_0 = \nu_s$, yielding the expression

$$\kappa(z) = 43.3 \mathrm{e}^{-(50.5)^2 (z - \frac{L}{2})^2}. \tag{6}$$

This function and the corresponding filter spectral response is shown in Fig. 2, with $\delta\nu = \nu_0 - \nu_s$ and the power conversion efficiency $E = |T(\omega)|^2$. The sidelobes in the filter's spectral response were suppressed to the extent that, for $|\delta\nu| \ge 100$ GHz, the transmittance is < -30 dB.

Table 1 shows the crosstalk calculated for channel center frequencies separated by $100m$ GHz from the carrier frequency, for $m = 1, 2$, and 3. Worst-case crosstalk levels below -30 dB were achieved at data rates to 20 Gb/s. And all insertion losses remain low (< -0.20 dB), which is acceptable for practical use.

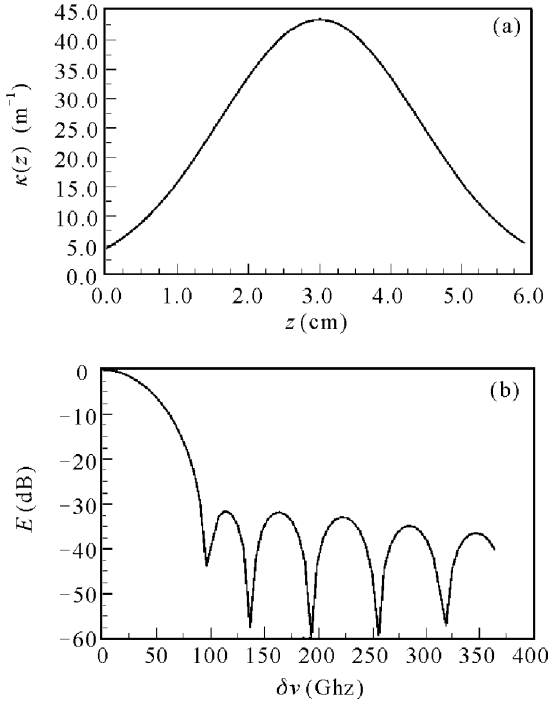

Fig. 2. (a) Spatial dependence of polarization coupling constant $\kappa(z)$ for Gaussian filter. (b) Spectral response for Gaussian filter.

Table 1. Crosstalk and Insertion Loss for Gaussian Apodizing Function

Data Rate	Crosstalk (dB)			Insertion
(Gb/s)	$m = 1$	$m = 2$	$m = 3$	Loss (dB)
2.5	−44.0	−41.9	−37.9	−0.05
10	−37.6	−41.0	−37.9	−0.08
20	−30.9	−39.1	−37.8	−0.20

In practical case, the stability of the laser carrier frequency ν_0 and the filter's selected frequency ν_s is required. It would be necessary to control both to the order of ± 1 GHz. This is commonly done with today's distributed feedback lasers using a thermoelectric cooler and thermistor in a feedback loop.

A half-tone technique is suggested as a means of achieving a desired apodizing profile $\kappa(z)$. In the case of the EOTF considered here, spatial period of the filter at the center of the active region can be calculated by $\lambda/(n_1 - n_3)$, with n_1 and n_3 the ordinary and extraordinary refractive indices of the waveguide material. Since the birefringence $(n_1 - n_3)$ of $LiNbO_3$ at room temperature for the wavelength of 1.53 μm is 0.079, a fully populated design would have 515 stripes per cm. From Fig. 2, it is evident that the minimum density of stripes would be about 50 per cm. This should be adequate to achieve a good performance for the tapered coupling.

In conclusion, a design of apodizing function for EOTF has been analyzed. Crosstalk level below -30 dB for data rates to 20 Gb/s and 100-GHz channel spacing are predicted for Gaussian apodizing function, assuming a 6-cm length for the polarization coupling/electrooptic tuning

region. The calculated insertion loss is also quite low. Thermal stabilization of frequency characteristics of both the laser light sources and the filter will be needed to achieve these results. A half tone lithography technique is suggested as a means of achieving desired apodizing function profiles. Other forms of apodizing functions can also be optimized by the same way as we did in this paper.

Special thanks to my respectable supervisor, Dr. Henry F. Taylor, professor of Texas A&M University of U. S., for his guidance.

This work was supported by the Scientific Research Foundation for the Returned Overseas Chinese Scholars, State Education Ministry. J. Zhou's e-mail address is jzhou2000@263.net.

References

1. F. Bolodeau, D. C. Johnson, S. Theriault, B. Malo, J. Albert, and K. O. Hill, IEEE Photon. Technol. Lett. **7,** 388 (1995).
2. L. Dong, P. Hua, T. A. Birks, L. Keekie, and P. St. J. Russell, IEEE Photon. Technol. Lett. **8,** 1656 (1996).
3. K. Hsu, C. M. Miller, and Y. Bao, Appl. Opt. **33,** 6617 (1994).
4. L. Stone and L. W. Stulz, Electron. Lett. **27,** 2239 (1991).
5. C. Dragone, IEEE Photonics Technol. Lett. **3,** 812 (1991).
6. C. Dragone, J. Lightwave Technol. **16,** 1895 (1998).
7. E. L. Wooten, R. L. Stone, E. W. Miles, and E. M. Bradley, J. Lightwave Technol. **14,** 2530 (1996).
8. C. Kostrzewa, R. Moosburger, G. Fischbeck, B. Schüppert, and K. Petermann, IEEE Photon. Technol. Lett. **9,** 1487 (1996).
9. F. Tian, C. Harizi, H. Herrmann, V. Reimann, R. Richen, V. Rust, W. Sohler, F. Wehrmann, and S. Westenhöfer, J. Lightwave Technol. **12,** 1192 (1994).
10. D. A. Smith, R. S. Chakravarthy, Z. Bao, J. E. Baran, J. L. Jackel, A. d'Alessandro, D. J. Fritz, S. H. Huang, X. Y. Zou, S.-M. Hwang, A. E. Willner, and K. D. Li, J. Lightwave Technol. **14,** 1005 (1996).
11. W. Warzanskyi, F. Heismann, and R. C. Alferness, Appl. Phys. Lett. **53,** 13 (1988).
12. Z. Tang, O. Eknoyan, H. F. Taylor, Electron. Lett. **30,** 1758 (1994).
13. H. F. Taylor and A. Yariv, Proc. IEEE **62,** 1044 (1974).
14. G. D. Boyd, W. L. Bond, and H. L. Carter, J. Appl. Phys. **38,** 1941 (1967).